# Lamellar Organic Thin Films through Self-Assembly and Molecular Recognition

Simon J. Holder,*[†,‡] Johannes A. A. W. Elemans,[†] Jack J. J. M. Donners,[†]
Mark J. Boerakker,[†] René de Gelder,[§] Joaquín Barberá,[||] Alan E. Rowan,[†] and
Roeland J. M. Nolte*[†]

*Department of Organic Chemistry, NSR Center, University of Nijmegen, Toernooiveld,
6525 ED Nijmegen, The Netherlands, Centre for Materials Research, University of Kent,
Canterbury, Kent, UK CT2 7NR, United Kingdom, Department of Inorganic Chemistry, NSR Center,
University of Nijmegen, and Química Orgánica, Facultad de Ciencias-ICMA, Universidad de
Zaragoza-CSIC, E-50009 Zaragoza, Spain*

*nolte@sci.kun.nl*

Molecular clips possessing U-shaped cavities have been functionalized on their convex side with long aliphatic tails. These molecules form dimers which self-assemble into malleable lamellar thin films. Upon addition of a guest (methyl 3,5-dihydroxybenzoate), a 1:1 host−guest complex is formed, which prohibits clip dimerization. As a result, the lamellar structure of the material is lost. Complexation of 3,5-dihydroxybenzoic acid in the clip results in host−guest complexes which dimerize by hydrogen bonding interactions between the carboxylic acid functions of the bound guests. This dimerization restores the lamellar type architecture of the material.

## Introduction

The design and construction of synthetic materials with a precise 2D or 3D architecture is an area of great interest. Several routes toward such materials can be followed, the most recent ones make use of molecular recognition processes.[1,2] The rational design of organized molecular materials is also a fundamental problem in crystal engineering.[3,4] In theory, since most organic compounds are crystalline, the identification of factors leading to different crystal structures would allow for the generation of a vast range of organic materials. In practice, however, the molecular interactions that generate certain crystal structures are multitudinous and the interpretation of the factors responsible for solid-state self-assembly is very difficult.[3,5] The rational design of materials becomes even more complicated when two or more distinct molecules are desired in a given solid-state structure.[6] In many cases, this is an elusive process

involving accommodation of small guest molecules into a porous crystalline host through rather unselective interactions.[7] It is therefore of particular interest to design and develop materials in which the different constituting building blocks are oriented in the crystal by making use of well-defined and directed intermolecular interactions, e.g., hydrogen bonds and π−π stacking. Excellent examples of such predesigned solid materials are Aoyama's stacked columns[8] and Wuest's networks,[9] which both contain small cavities with directed functional groups in which guest molecules can be complexed. Other well-defined cavity-containing crystals are those formed by Ghadiri's cyclic peptides,[10] whereas Gin has constructed polymerizable liquid-crystalline nanocomposites containing compartments that can accommodate metal complexes. In the latter example the enclosed metal complexes exhibited unique physical properties different to those of the complexes in the bulk or in solution.[11] In addition to these open-framework materials, many lamellar or layered solids are known which possess a spatial ordering of the molecular components in two dimensions.[7,12] It is of great interest to design similar materials

[†] Department of Organic Chemistry, NSR Center, University of Nijmegen.
[‡] Centre for Materials Research, University of Kent.
[§] Department of Inorganic Chemistry, NSR Center, University of Nijmegen.
Química Orgánica, Facultad de Ciencias-ICMA, Universidad de Zaragoza.

(1) Lehn, J.-M. *Supramolecular Chemistry − Concepts and Perspectives*; VCH: Weinheim, 1995, Chapter 9 and references therein.
(2) (a) Whitesides, G. M.; Mathias, J. P.; Seto, C. T. *Science* **1991**, *254*, 1312. (b) Martin, C. R. *Chem. Mater.* **1996**, *8*, 1739. (c) Stupp, S. I.; Braun, P. V. *Science* **1997**, *277*, 1225.
(3) Desiraju, G. R. *Crystal Engineering: The Design of Organic Solids*; Elsevier: Amsterdam, 1989.
(4) Reviews: (a) Gavezotti, A. *Acc. Chem. Res.* **1994**, *27*, 309. Russell, V. A.; Ward, M. D. *Chem. Mater.* **1996**, *8*, 1654. (b) Desiraju, G. R. *Chem. Commun.* **1997**, 1475. (c) Ashton, P. R.; Fyfe, M. C. T.; Hickingbottom, S. K.; Menzer, S.; Stoddart, J. F.; White, A. J. P.; Williams, D. J. *Chem. Eur. J.* **1998**, *4*, 577.
(5) (a) Lehn, J.-M. *Angew. Chem., Int. Ed. Engl.* **1990**, *29*, 1304. (b) Garcia-Tellado, F.; Geib, S. J.; Goswami, S.; Hamilton, A. D. *J. Am. Chem. Soc.* **1991**, *113*, 9265. (c) Mathias, J. P.; Stoddart, J. F. *Chem. Soc. Rev.* **1992**, *21*, 215. (d) Aakeröy, C. B.; Hughes, D. P.; Niewenhuyzen, M. *J. Am. Chem. Soc.* **1996**, *118*, 10134.

(6) Bishop, R. *Chem. Soc. Rev.* **1996**, *25*, 311.
(7) Mallouk, T. E.; Gavin, J. A. *Acc. Chem. Res.* **1998**, *31*, 209.
(8) (a) Endo, K.; Sawaki, T.; Koyanagi, M.; Kobayashi, K.; Masuda, H.; Aoyama, Y. *J. Am. Chem. Soc.* **1995**, *117*, 8341. (b) Aoyama, Y.; Endo, K.; Anzai, T.; Yamaguchi, Y.; Sawaki, T.; Kanehisa, N.; Hashimoto, H.; Kai, Y.; Masuda, H. *J. Am. Chem. Soc.* **1996**, *118*, 5562, (c) Dewa, T.; Endo, K. Aoyama, Y. *J. Am. Chem. Soc.* **1998**, *120*, 8933.
(9) Brunet, P.; Simard, M.; Wuest, J. D. *J. Am. Chem. Soc.* **1997**, *119*, 2737.
(10) (a) Ghadiri, M. R.; Granja, J. R.; Milligan, R. A.; McRee, D. E.; Khazanovich, N. *Nature* **1993**, *366*, 324. (b) Kim, H. S.; Hartgerink, J. D.; Ghadiri, M. R. *J. Am. Chem. Soc.* **1998**, *120*, 4417. (c) Vollmer, M. S.; Clark, T. D.; Steinem, C.; Ghadiri, M. R. *Angew. Chem., Int. Ed.* **1999**, *38*, 1598.
(11) (a) Smith, R. C.; Hu, S.; Juang, E.; Gin, D. L. *J. Am. Chem. Soc.* **1997**, *119*, 4092. (b) Gray, D. H.; Gin, D. L. *Chem. Mater.* **1998**, *10*, 1827. (c) Deng, H.; Smith, R. C.; Gin, D. L. *J. Am. Chem. Soc.* **1998**, 3522. (d) Miller, S. A.; Kim, E.; Gray, D. H.; Gin, D. L. *Angew. Chem., Int. Ed.* **1999**, *38*, 3022.

**Chart 1**
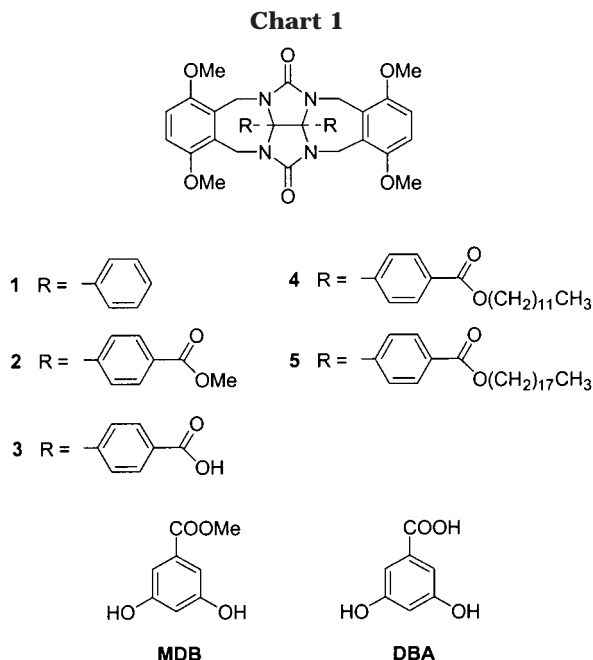


in which guest molecules can be incorporated at discrete positions in the layers. A wide array of potential applications for such lamellar host−guest materials can be envisaged, e.g., in photovoltaic or condensator-like devices.

This paper describes our initial efforts toward the construction of host−guest materials, by the lamellar self-assembly of host molecules which can recognize small guests by hydrogen bonding and $\pi-\pi$ stacking interactions. Over the past decade we have been studying a class of host compounds commonly referred to as "molecular clips".[13] These molecules of type **1** (Chart 1) possess a rigid, U-shaped cavity in which 1,3-dihydroxybenzene guests can be selectively bound in a 1:1 host−guest ratio (Figure 1a).[14] It is only recently that a further aspect of these molecules revealed itself: they can form dimers in organic solution and in the solid state, in which the cavity of one molecule is filled by the side-wall of its dimeric partner and vice-versa (Figure 1b). In aqueous solution, water-soluble clip molecules can assemble in this way to form well-defined nano-arrays.[15]

Stimulated by this dimeric self-association phenomenon we decided to derivatize molecular clips at their convex side with long aliphatic tails, the concept being that these molecules could dimerize to form smectic liquid-crystals, due to the resemblance of such a dimer to a rodlike mesogen (Figure 1c). In analogy to many crystal structures of clip molecules, it was expected that these dimers would further organize themselves as a result of $\pi-\pi$ interactions between the clip headgroups and thus form lamellar arrays. By the binding of 1,3-dihydroxybenzene guest molecules into the clips, it was
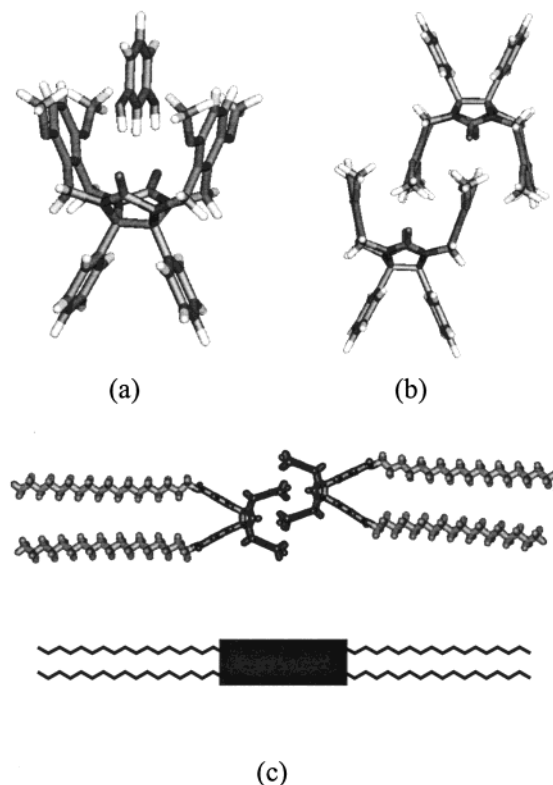


**Figure 1.** (a) Structure of the complex between molecular clip **1** and a 1,3-dihydroxybenzene guest. (b) Dimeric structure formed by two molecules of **1**. (c) Computer-modeled picture of a dimer of two clips with long aliphatic tails (top) and the analogy with the structure of a rodlike mesogen (bottom).

hoped that they would be included in the material and hence alter its properties. In this paper, we report on the synthesis and materials properties of these new clip molecules and their host−guest complexes in some detail.[16]

## Results and Discussion

**Synthesis.** Starting from dicarboxylic acid derivative **3**,[17] clip molecules **4** and **5** were prepared in yields of 73 and 82%, respectively, by esterification with the appropriate 1-bromoalkane in DMF, using $K_2CO_3$ as a base (Chart 1). Both **4** and **5** were fully characterized by FTIR, ^{1}H and ^{13}C NMR, electrospray mass spectroscopy, and elemental analysis.

**Thermal Behavior of Clips 4 and 5.** Analysis of a sample of **4** with polarizing microscopy (PM) showed that a birefringent texture evolved upon cooling from the isotropic melt. Two different textures were observed: a highly colored, polychromatic one with no clearly defined pattern, although a spherulitic texture was often visible, and a platelet/mosaic texture[18] reminiscent of a smectic

(12) (a) Lee, K. M.; Lee, C. K.; Lin, I. J. B. *Angew. Chem., Int. Ed. Engl.* **1997**, *36*, 1850. (b) Sharma, C. V. K.; Bauer, C. B.; Rogers, R. D.; Zaworotko, M. J. *Chem. Commun.* **1997**, 1559.

(13) Review: Rowan, A. E.; Elemans, J. A. A. W.; Nolte, R. J. M. *Acc. Chem. Res.* **1999**, *32*, 995.

(14) Reek, J. N. H.; Priem, A. H.; Engelkamp, H.; Rowan, A. E.; Elemans, J. A. A. W.; Nolte, R. J. M. *J. Am. Chem. Soc.* **1997**, *119*, 9956.

(15) (a) Reek, J. N. H.; Kros, A.; Nolte, R. J. M. *Chem. Commun.* **1996**, 245. (b) Elemans, J. A. A. W.; de Gelder, R.; Rowan, A. E.; Nolte, R. J. M. *Chem. Commun.* **1998**, 1553.

(16) Part of this work has been published as a preliminary communication: Holder, S. J.; Elemans, J. A. A. W.; Barberá, J.; Nolte, R. J. M. *Chem. Commun.* **2000**, 355.

(17) Elemans, J. A. A. W.; Slangen, R. R. J.; Rowan, A. E.; Nolte, R. J. M. Manuscript in preparation.

(18) The platelet texture was predominantly observed when the film was thinner. Strong evidence that both textures result from the same crystal structure comes from the fact that their melting and crystallization temperatures are the same. Further evidence is that the polychromatic texture often merges with the platelet texture in the same sample, particularly at the sample edges where the sample is thinner.
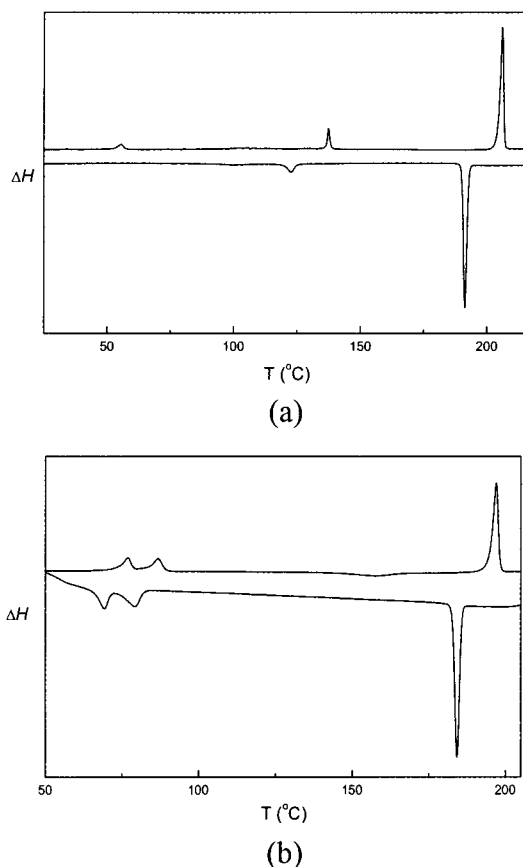
(a)



(b)

**Figure 2.** (a) DSC thermogram of **4.** (b) DSC thermogram of **5**.

**Table 1. Phase Transition Temperatures and Enthalpies of Clips 4 and 5 and Their 1:1 Complexes with MDB and DBA Guests As Observed by DSC**

| clip or complex | transition[a] | $T\,(°C)^{b}$ | $\Delta H\,(kJ\;mol^{-1})^{b}$ |
|---|---|---|---|
| **4** | $K \to K^{1}$ | 137.6 (122.6) | 3.0 (−2.9) |
| | $K^{1} \to I$ | 206.0 (191.4) | 25.3 (−23.6) |
| **5** | $K \to K^{1}$ | 36.1 (−)$^{c}$ | 5.2 (−)$^{c}$ |
| | $K^{1} \to K^{2}$ | 79.6 (73.7) | 10.4 (−10.0) |
| | $K^{2} \to K^{3}$ | 89.7 (83.9) | |
| | $K^{3} \to I$ | 195.4 (185.6) | 21.3 (−15.2) |
| **4:MDB** | $K \to I$ | 130.2 (67.6) | 32.1 (−8.5) |
| **5:MDB** | $K \to I$ | 107.3 (53.2) | 19.4 (−16.7) |
| **5:DBA** | $K \to I$ | 170.1 (137.2) | 32.4 (−28.8) |

[a] K, $K^{1}$, $K^{2}$, $K^{3}$ = crystalline phases; I = isotropic phase. [b] Values obtained from the second heating run; in parentheses the values obtained from the first cooling run. [c] No phase transition was observed.

liquid-crystalline mesophase.[19] Upon cooling, between 191 and 122 °C liquid crystalline-like behavior was observed in the sense that the birefringence was maintained, and in addition the material was malleable and sheerable when pressure was applied. Prolonged or increased pressure often was found to lead to a certain degree of flow, and small crystallites surrounded by thin layers of isotropic fluid were observed, suggesting that localized melting occurred. Below 122 °C, the texture was retained but the material was now completely solid.

Differential scanning calorimetry (DSC) studies (Figure 2a, Table 1) showed a phase transition at 122.6 °C in the cooling run coinciding with the observed solidifica-

**Table 2. d-Spacings Corresponding to Lamellar Thicknesses Observed for Compound 5 and Its Complexes with MDB and DBA**

| clip or complex (1:1 host−guest) | $T\,(°C)$ | lamellar thickness (Å) |
|---|---|---|
| **5** | 20$^{a}$ | 38.6 |
| | 20$^{b}$ | 28.1 |
| | 130 | 40.9 |
| | 175 | 41.6 |
| **5:MDB** | 20$^{a}$ | 37.5 |
| | 20$^{b}$ | −$^{c}$ |
| **5:DBA** | 20$^{a}$ | 37.5 |
| | 20$^{b}$ | 57.2 |

[a] Freshly prepared sample. [b] After recrystallization of the sample from the melt. [c] No d spacing observed.

tion of the texture by PM. The (second) heating run revealed the inverse of the cooling behavior, the material becoming malleable again at 137.6 °C up to isotropization at 206 °C. The enthalpy involved with this last transition was, however, far larger than would have been expected for a mesophase to isotropic liquid transition, suggesting that the material is in fact *crystalline* throughout the whole temperature range. This was confirmed by variable temperature X-ray powder diffraction (XRPD) studies, which showed numerous reflections in the middle to high angle regions, indicative of typical three-dimensional crystalline phases. This reflection pattern changed with increasing temperature, indicating a crystal−crystal transition, but no pattern ascribable to a mesophase became evident.

By enlarging the aliphatic tails it was hoped that liquid crystalline behavior would be induced. Upon cooling compound **5**, which has two octadecyl tails, from the melt, two textures were observed by PM which were both very similar to those observed for **4**. Both textures were again malleable over a wide temperature range, viz. from 185 to 84 °C upon cooling and from 90 to 195 °C upon heating. At lower temperatures, the birefringence remained but the material was solid.

The large $\Delta H$ value observed by DSC corresponding to the isotropic melt transition at 195.4 °C in the heating run (Figure 2b, Table 1) suggested that **5**, like **4**, exhibited no mesogenic behavior. The transition from malleable to solid phase in the cooling run at 84 °C, as observed with PM, coincided with the first of three exotherms in the DSC trace, while the following heating run showed the inverse of the cooling behavior.[20] XRPD studies confirmed the crystalline nature of the material up to isotropization. A change in the reflection pattern also confirmed at least one crystal−crystal transition between 20 and 100 °C. More importantly, however, unlike in the case of **4**, for **5** a set of equally spaced reflections (corresponding to first, second, third etc. order reflections) in the low-angle region of all patterns between room temperature and melting was observed, indicating that **5** possessed a layered structure. The lamella thickness increased from 28.1 Å at 20 °C to 40.9 Å at 130 °C, with a further slight increase to 41.6 Å at 175 °C (Table 2).

**Ordering of the Clips.** The textures observed for **4** and **5** indicate long-range ordering of the molecules in

(19) Gray, G. W.; Goodby, J. W. G. *Smectic Liquid Crystals − Textures and Structures*; Leonard Hill: Glasgow, 1984.

(20) The exotherm observed at 162 °C in the heating run is due to a cold crystallization, caused by incomplete crystallization in the cooling run because of too rapid cooling (10 °C min$^{-1}$). No exotherm was visible in the heating run when the sample was cooled at lower rates (1 °C min$^{-1}$) from the isotropic melt.

(a)



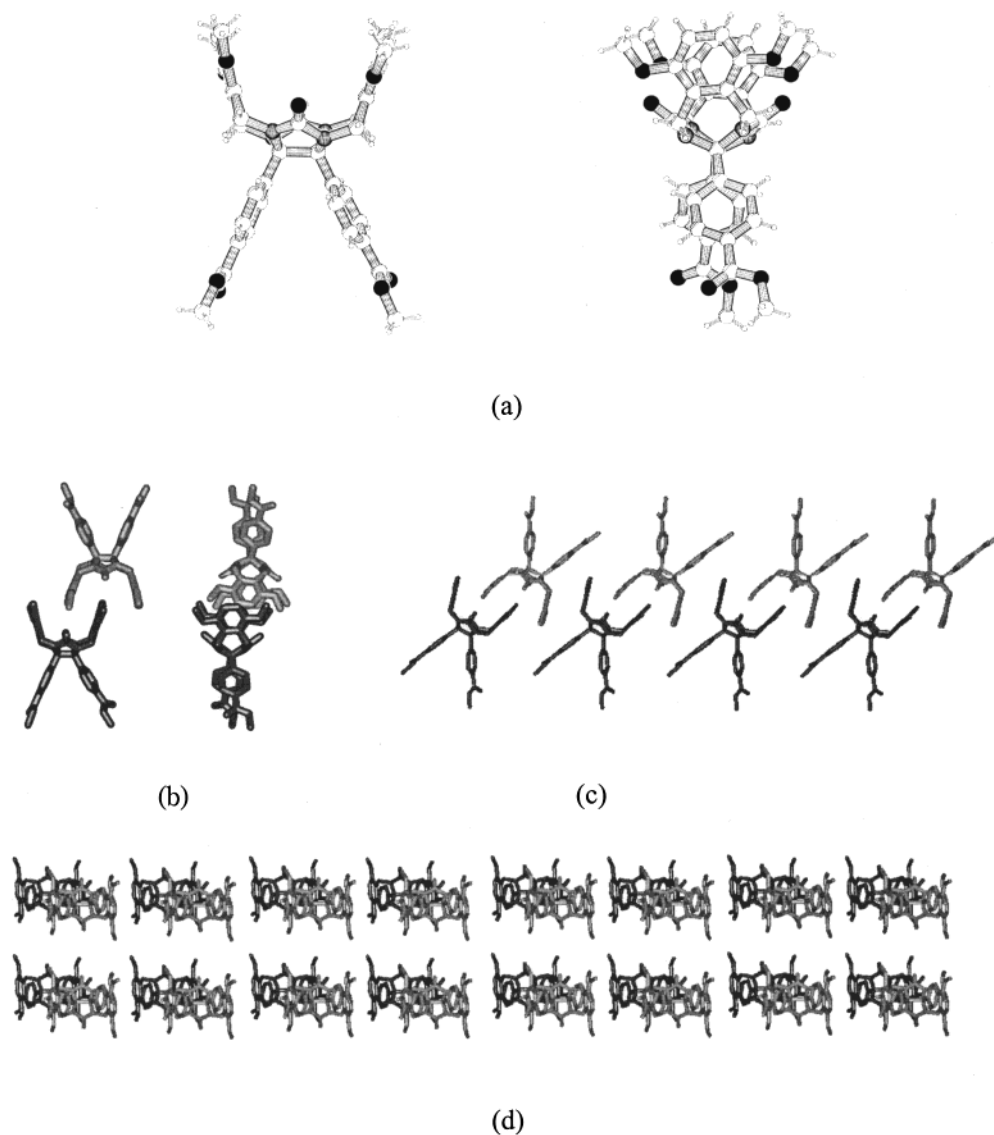(b)                                        (c)



(d)

**Figure 3.** Ordering of clips in the X-ray structure of **2**. (a) Front and side view of the molecular structure of **2**. (b) Front and side-view of a dimer of **2**. (c) Front view of an array of dimers of **2**. (d) Top view of two arrays of dimers of **2**.

the solid state. To the best of our knowledge, the polychromatic texture cannot be assigned to a known structure; the spherulites, however, are indicative of a lamellar organization.[21] The more commonly observed platelet structures are highly characteristic of a smectic organization in the thin films, and the observation of relatively large domains indicates long-range ordering (approaching several millimeters).

A model for the organization of the clips within the layers can be derived on the basis of the structure of the methyl ester compound **2**, which was solved by X-ray analysis (Figure 3a). In the crystalline state, clip **2** exists as discrete, slightly offset dimers, in which the cavity of one clip is filled by the side-wall of a partner (Figure 3b).

This is in contrast to the crystal structure of **1**,[22] in which the molecules are not arranged in discrete dimers, but in sheets of clips giving an interwoven network (Figure 4) which is stabilized by $\pi-\pi$ stacking interac-

tions between the clip layers. In the case of **2**, $\pi-\pi$ interactions between the aromatic rings of the side-walls in adjacent dimers give rise to chains of clips which further self-assemble to yield sheetlike structures (Figure 3c,d). It is relatively easy to envisage how the extension of the ester methyl group to an octadecyl chain would give rise to a bilayer of clip molecules, surrounded by aliphatic tails. This bilayer model is depicted in Figure 5 and is supported by the XRPD measurements on compound **5**. The lamellar thickness of 28.1 Å at 20 °C can be explained by the presence of dimers which are tilted at an angle of at least 40° and have fully interdigitated alkyl chains.[23] The increase in layer spacing to 40.9 (130 °C) and 41.6 Å (175 °C) at higher temperatures is in good agreement with the length of a tilted bilayer of dimers of **5** with almost no alkyl chain interdigitation.

To obtain more information about the precise mode of self-assembly of **5** in the solid state, cross polarization magic angle spinning (CPMAS) ^{13}C spectra of this

(21) Billmeyer, F. W., Jr. *Textbook of Polymer Science*; John Wiley and Sons: New York, 1984.

(22) Sijbesma, R. P.; Kentgens, A. P. M.; Lutz, E. T. G.; van der Maas, J. H.; Nolte, R. J. M. *J. Am. Chem. Soc.* **1993**, *115*, 8999.

(23) A similar tilting of the dimers is observed in the crystal structure of **2** (see Figure 3c).
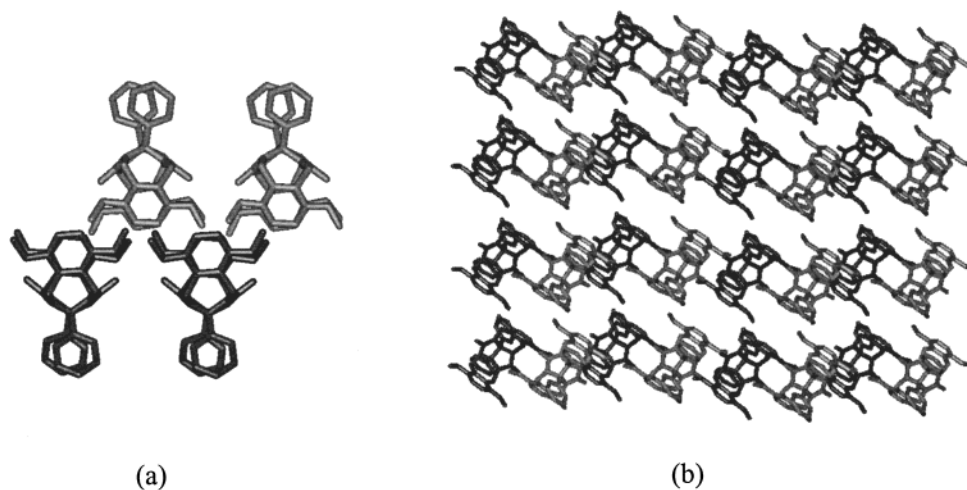
**Figure 4.** Ordering of clips in the X-ray structure of **1**. (a) Side-view of two dimers of **1**. (b) Top view of the interwoven network formed by **1**.
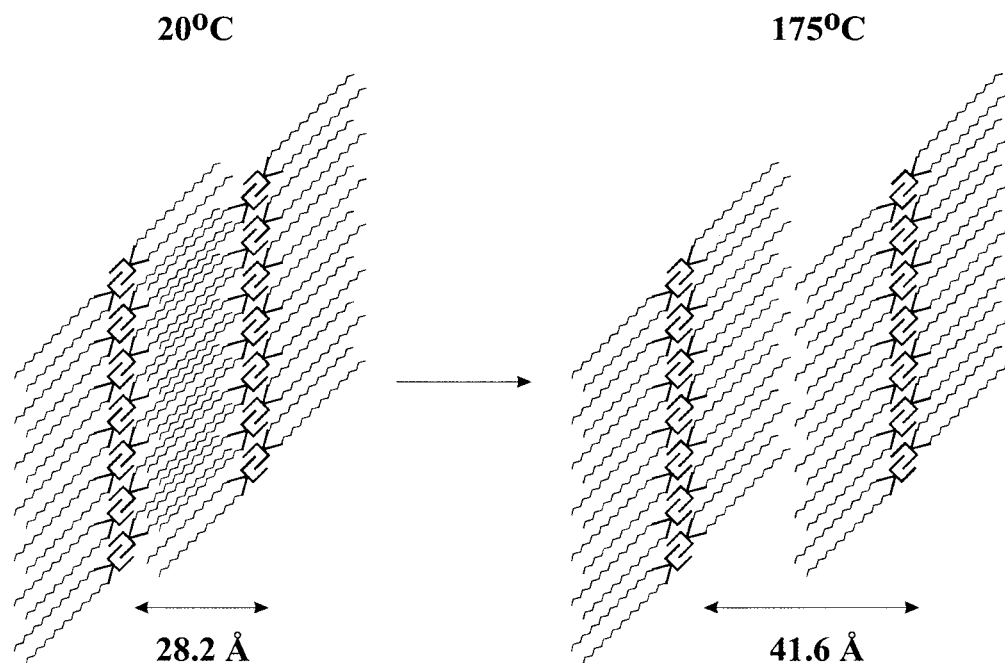


**Figure 5.** Bilayerlike ordering of the molecules of **5** at room temperature and in the malleable lamellar phase at 175 °C.

compound were recorded at 20 °C and at 150 °C (Figure 6). All carbon resonances of **5** in these spectra could be assigned using the corresponding $^{13}C$ and DEPT-135 solution spectra. The carbon nuclei expected to show the greatest difference in their magnetic environment, depending on the mode of dimerization, are the side-wall carbon atoms *e* and the methoxy carbon atoms *c*. Four signals for *e* and four signals for *c* can be expected if **5** exists in discrete, slightly offset dimers, as is the case in the solid-state structure of **2** (Figure 3). At 150 °C, this seems to be the case. At room temperature, however, for both *e* and *c* fewer signals are observed, indicating a higher degree of symmetry. At this temperature, the clips apparently do not exist as discrete dimers, but appear to have a more overlapping dimeric structure as observed in the crystal structure of clip **1** (Figure 4). The resulting interwoven structure then may account for the typically nonmalleable crystalline behavior at low temperatures, whereas the formation of discrete dimers at higher

temperatures would contribute to the induction of malleability. A further contribution to this malleability could be a decreased interdigitation of the alkyl tails at higher temperatures, as was suggested by the XRPD results. A downfield shift of the carbon nuclei at the termini of the aliphatic chains (*a*−*b*) upon going from 20 to 150 °C, indicating a deshielding of these atoms, is in agreement with this assumption. Furthermore, the decrease in the $CH_2$ main chain peak width at 150 °C is indicative of a higher degree of conformational mobility of the hydrocarbon tails.

The lamellar nature of **5** explains the malleability of the material at high temperatures as observed by PM. We attribute this behavior to the three above-mentioned factors (Figure 7): (i) above the crystal−crystal transition at 90 °C the fully interdigitated octadecyl tails become separated resulting in an increased lamella spacing; (ii) above this transition the octadecyl tails obtain an increased mobility, and (iii) the clip headgroups rearrange
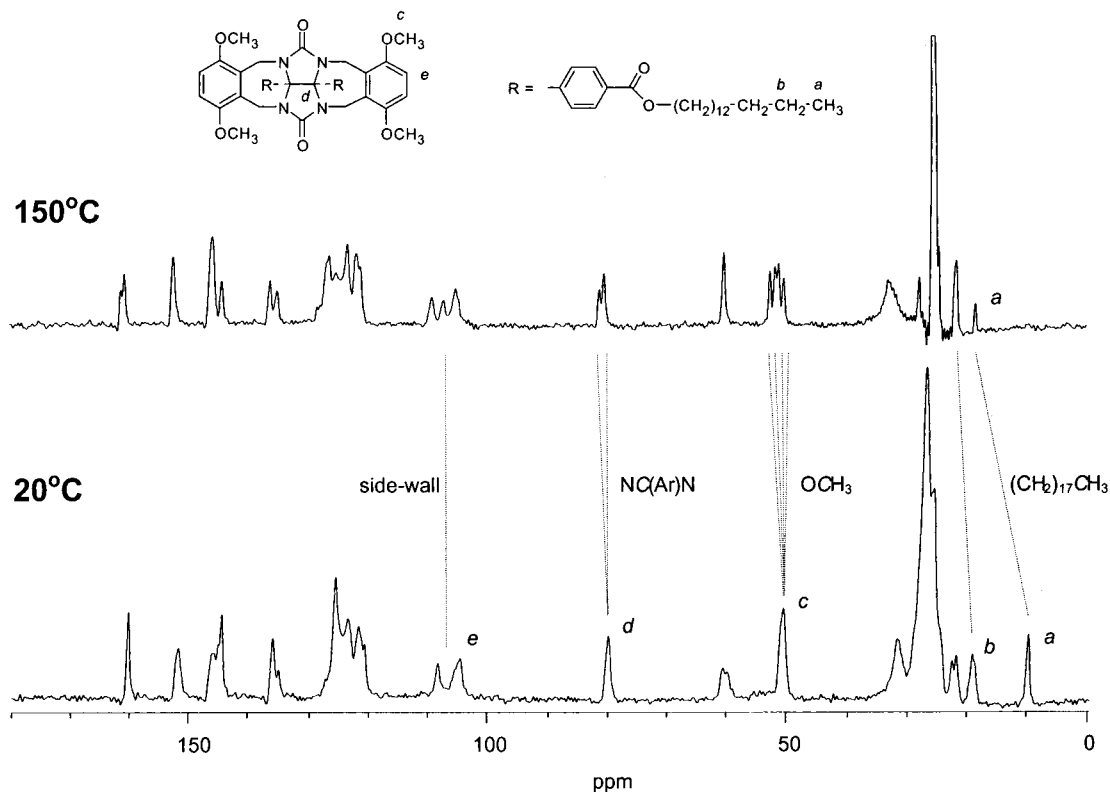
**Figure 6.** $^{13}$C CPMAS spectra of compound **5** at 150 and 20 °C.

from an interwoven structure to a structure with discrete dimers. All factors are expected to contribute to a weakening of the internal cohesion of the bilayers and as a result lead to an increased malleability of the material.[24] The partially separated layers can more readily slide over one another in a manner analogous to other layered materials, such as graphite and talcum powder.

**Host−Guest Complexes.** Since the above-mentioned bilayerlike ordering of clips **4** and **5** may be responsible for the lamellar nature of the material, it was of interest to investigate the consequences of disrupting the dimeric structure of the clips by adding dihydroxybenzene guest molecules. An equimolar mixture of **4** and methyl 3,5-dihydroxybenzoate (**MDB**, see Chart 1) was prepared by solvent evaporation of a solution of the two components in a chloroform−methanol mixture (4:1, v/v). It was expected that dimerization of the clips would now be prevented and that 1:1 host−guest complexes would be quantitatively formed.[25] The freshly prepared mixtures initially displayed phase separation by PM and DSC indicating that complex formation was incomplete. To encourage complete host−guest complexation, the mixture was first heated to isotropization and then slowly
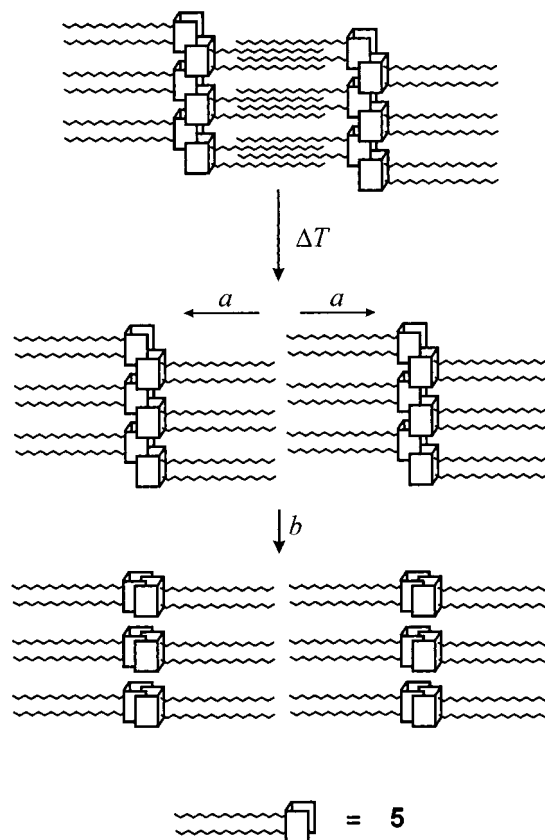
(24) Whereas a simple lamellar structure with weak interactions between clip bilayers explains the malleability of the material, it does not explain the appearance of an apparently isotropic fluid component which was observed upon the application of pressure. A possible explanation for this behavior could be that due to the applied pressure van der Waals attractions responsible for the bilayer cohesion are broken. Essentially without this self-assembly process, the monomers or dimers melt and form an isotropic liquid.

(25) This assumption is based on the known fact that in chloroform solution host−guest complexation prevents dimerization of the clip molecules. The association constant of the **5**:**MDB** complex is much higher ($K_a = 1 \times 10^4$ M$^{-1}$) than the dimerization constant ($K_{dimer} = 18$ M$^{-1}$) of **5**.



**Figure 7.** Schematic overview of the most important processes that take place when compound **5** is heated from 20 °C to 150 °C. (a) Separation of the alkyl tails, resulting in an increase in the lamellar distance. (b) Reorganization of the clip headgroups from an overlapped polymeric into a discrete dimeric structure.
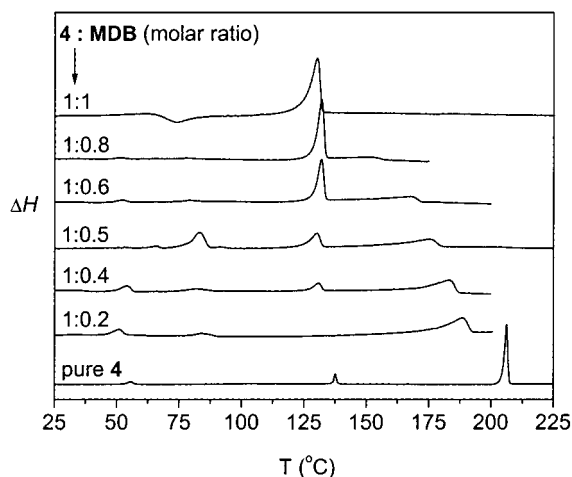
**Figure 8.** DSC traces of the heating runs of the complexes of **4** with various amounts of **MDB**.

cooled, whereupon at 68 °C a birefringent, nonmalleable microcrystalline texture began to appear typical of a crystalline organic material. Upon cooling, DSC analysis showed that a single exotherm at 67.6 °C was present, whereas an exotherm due to cold crystallization was visible in the consecutive heating run followed by a melting endotherm at 130 °C (top trace in Figure 8). The absence of phase separation in the mixture was concluded from both PM and DSC measurements, suggesting that a complete host–guest complex formation had taken place. This complexation should prevent dimerization of the clips and the formation of extended 2D sheets. As a result the energy required for melting is reduced leading to a dramatic reduction of the melting point, which was observed.

To confirm the formation of a 1:1 host–guest complex, varying ratios of **4** to **MDB** were prepared. The DSC traces of the second heating runs of these mixtures are shown in Figure 8. As is apparent, the incorporation of progressively lower quantities of **MDB** into the mixtures results in a gradual diminution of the melting endotherm of the 1:1 complex at 130 °C. Simultaneously, the appearance of a second endotherm at progressively higher temperatures displaying increasing enthalpies, attributable to uncomplexed **4**, becomes apparent. At a molar ratio of **4**:**MDB** = 1:0.5, stable crystals in an isotropic fluid became visible at 150 °C, indicative of a high degree of phase separation between uncomplexed **4** and the host–guest complex. The endotherms below 100 °C in Figure 8 are presumed to be crystal–crystal transitions unconnected with the phase separation between the host–guest complex and the free clip.

The thermal behavior of complexes of **5** and **MDB** was very similar to that of the complexes of **4** and **MDB**. Cooling of the 1:1 complex of **5** and **MDB** from the isotropic melt gave a nonmalleable birefringent microcrystalline texture at 53 °C, while the material melted at 107.3 °C in the following heating run. Whereas the FTIR spectrum of uncomplexed **5** displayed a vibration of the carbonyl group of the glycoluril core at 1722 cm⁻¹, that of the complex showed a shift of this stretching vibration to 1718 cm⁻¹, indicative of a hydrogen bonding interaction between **5** and the **MDB** guest. More importantly, the absorption due to the OH stretching vibration of the **MDB** guest narrowed considerably upon complexation and shifted from 3387 to 3337 cm⁻¹, again indicating

hydrogen bonding. The nature of this 1:1 complex was further investigated with XRPD (Table 2). The diffractogram at 20 °C obtained for the mixture directly after solvent evaporation displayed numerous reflections many of which were similar in position to those observed for uncomplexed **5**. In addition, *d* spacings corresponding to a lamellar thickness of 37.5 Å were observed in the low-angle region. After recrystallization of the mixture from the melt, a unique diffraction pattern was observed which showed no peaks in the low-angle region anymore, indicating the disappearance of the lamellar structure of **5**.

If **MDB** prevents **4** and **5** to form dimers and adopt a lamellar organization, complexation of a guest which again allows dimerization of the resulting host–guest complex should in principle restore the lamellar behavior. To investigate this, the 1:1 complex of **5** and 3,5-dihydroxybenzoic acid (**DBA**, see Chart 1) was prepared. This guest can complex with its phenolic hydroxy groups to the carbonyl groups of **5**, and additionally form a dimer with another clip-bound **DBA** guest via its carboxylic acid group. Upon cooling from the melt, the complex of **5** and **DBA** displayed a clearly spherulitic birefringent texture at 137 °C. As for uncomplexed **5**, the film of the complex was malleable. This property disappeared below 100 °C when a typical crystalline solid behavior was observed. Unlike in the case of uncomplexed **5**, no clear transition from solid crystal to malleable crystal was visible by DSC which would correlate with the PM observations. XRPD measurements on the freshly prepared sample revealed many reflections which coincided with those observed for uncomplexed **5**. After recrystallization from the melt a unique pattern was observed, which showed reflections in the small angle region arising from first-, second-, and third-order reflections corresponding to a lamellar thickness of 57.2 Å. This value is in agreement with an "extended dimer" structure as depicted in Figure 9. Further evidence for this structure comes from the FTIR spectrum of the complex. As for the complex of **5** with **MDB**, the complex with **DBA** showed a single urea carbonyl stretching vibration at 1718 cm⁻¹ indicative of a hydrogen bonding interaction between the host and the guest. The absorption due to the OH stretching vibration of the hydroxyl groups of the **DBA** guest narrowed considerably upon complexation and shifted from 3327 to 3302 cm⁻¹, again indicating hydrogen bonding interactions with **5**. Most importantly, however, the carbonyl stretching vibration at 1690 cm⁻¹ due to the dimeric benzoic acid structure was preserved in the crystalline complex.

### Conclusion

The attachment of long alkyl tails to the convex side of molecular clips derived from glycoluril leads to interesting self-assembled architectures. The molecules adopt a bilayer structure through a mutual cavity filling process (dimerization) which in combination with intermolecular π–π stacking interactions generate malleable crystalline thin films. Between room temperature and melting to the isotropic liquid state the clip compounds undergo a number of crystal–crystal phase transitions. The last transition results in a lamellar crystalline phase which displays a malleable behavior.

Host–guest complexes of the clip molecules can be generated by melt-processing stoichiometric quantities
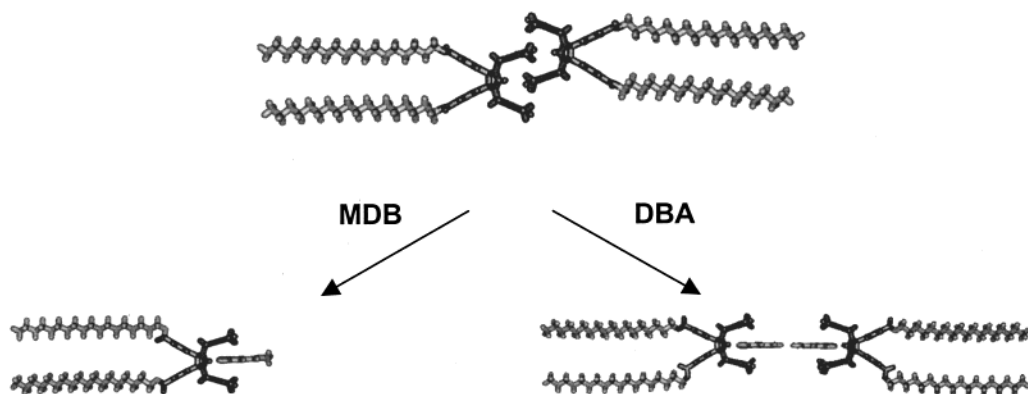
**Figure 9.** Computer-modeled pictures of the 1:1 host−guest complexes of **5** with **MDB** and **DBA**.

of the clip and hydroxy-substituted aromatic guest molecules, like **MDB** and **DBA**. Upon complexation, the former guest disrupts the self-assembly process of the clip molecules. As a result the bilayer structure is disrupted and a simple crystalline solid with no higher structural order is generated. When complexed with **DBA**, the clip molecules again can self-assemble, viz. through the formation of acid dimers. The consequence of this process is that the bilayer structure is restored and that the material becomes malleable again. Further research into the self-assembling properties of the molecular clips will focus upon the introduction of functional guests into the layered structures and the induction of real liquid-crystalline properties. The latter is hoped to be accomplished by increasing the volume of the aliphatic tails, resulting in a weakening of the interdimer interactions and thus a disruption of the 2D layers. Work along this line is in progress.

## Experimental Section

**Materials and Methods.** DMF was dried over BaO for one week and then vacuum distilled. $K_2CO_3$ was dried in an oven (150 °C). All other chemicals were commercial products and used as received. Molecular modeling calculations were performed on a Silicon Graphics Indigo II work station using the CHARMm force field.[26]

**Syntheses.** Compound **1** was synthesized as described in the literature.[27] The synthesis of compounds **2** and **3** will be described elsewhere.[17]

**5,7,12,13b,13c,14-Hexahydro-1,4,8,11-tetramethoxy-13b,-13c-bis(4-dodecoxycarbonyl)phenyl)-6*H*,13*H*-5a,6a,12a,-13a-tetraazabenz[5,6]azuleno[2,1,8-*ija*]benz[*f*]azulene-6,13-dione (4).** Compound **3** (200 mg, 0.283 mmol), 1-bromododecane (285 mg, 1.71 mmol), $K_2CO_3$ (400 mg, 4.27 mmol), and KI (5 mg) were added to degassed DMF (10 mL) and stirred under nitrogen at 100 °C for 64 h. After cooling, the mixture was evaporated to dryness, and the residue was dissolved in $CH_2Cl_2$ (100 mL). This solution was washed with aqueous 1 N HCl (2 × 100 mL) and with water (200 mL) and evaporated to dryness. The residue was recrystallized from a mixture of $CH_2Cl_2$ and ethanol (1:9, v/v) to yield 215 mg (73%) of **4** as a white powder.

Mp 206 °C; IR (KBr pellet) $\nu$ = 2980−2840, 1722, 1576, 1559, 1540, 1486, 1459, 1438, 1425, 1307, 1264, 1218, 1108, 1080 cm$^{-1}$; $^1$H NMR (300.13 MHz, CDCl$_3$) $\delta$ = 7.77 (d, 4H, $^3J$ = 8.4 Hz), 7.17 (d, 4H, $^3J$ = 8.4 Hz), 6.45 (s, 4H), 5.56 (d, 4H, $^2J$ = 15.9 Hz), 4.24 (t, 4H, $^3J$ = 6.7 Hz), 3.73 (d, 4H, $^2J$ = 15.9

Hz), 3.71 (s, 12H), 1.79−1.67 (m, 4H), 1.44−1.17 (m, 36H), 0.88 (t, 6H, $^3J$ = 6.4 Hz) ppm; $^{13}$C{$^1$H} NMR (75.47 MHz, CDCl$_3$) $\delta$ = 165.85, 157.56, 150.91, 139.09, 130.77, 129.81, 128.16, 126.91, 111.83, 84.90, 65.40, 56.64, 36.92, 31.89, 29.51, 29.32, 28.57, 25.95, 22.67, 14.10 ppm; ESI-MS $m/z$ 1043.9 (M$^+$), 1065.6 (M + Na$^+$), 2109.4 (M + M + Na$^+$). C$_{62}$H$_{82}$N$_4$O$_{10}$: calcd C, 71.37, H, 7.92, N, 5.37; found C, 71.34, H, 7.97, N, 5.35.

**5,7,12,13b,13c,14-Hexahydro-1,4,8,11-tetramethoxy-13b,-13c-bis(4-octadecoxycarbonyl)phenyl)-6*H*,13*H*-5a,6a,12a,-13a-tetraazabenz[5,6]azuleno[2,1,8-*ija*]benz[*f*]azulene-6,13-dione (5).** This compound was synthesized as described for **4** starting from **3** (300 mg, 0.425 mmol), 1-bromooctadecane (566 mg, 1.70 mmol), $K_2CO_3$ (590 mg, 4.27 mmol), and KI (5 mg) dissolved in DMF (15 mL). Yield 420 mg (82%) of **5** as a white powder.

Mp 195 °C; IR (KBr pellet) $\nu$ = 2960−2840, 1720, 1611, 1597, 1577, 1487, 1468, 1438, 1425, 1407, 1305, 1275, 1266, 1120, 1106, 1077 cm$^{-1}$; $^1$H NMR (300.13 MHz, CDCl$_3$) $\delta$ = 7.76 (d, 4H, $^3J$ = 8.5 Hz), 7.17 (d, 4H, $^3J$ = 8.5 Hz), 6.54 (s, 4H), 5.55 (d, 4H, $^2J$ = 15.9 Hz), 4.23 (t, 4H, $^3J$ = 6.7 Hz), 3.76 (d, 4H $^2J$ = 15.9 Hz), 3.74 (s, 12H), 1.70 (m, 4H), 1.45−1.19 (m, 60H), 0.88 (t, 6H, $^3J$ = 6.4 Hz) ppm; $^{13}$C{$^1$H} NMR (75.47 MHz, CDCl$_3$) $\delta$ = 165.83, 157.55, 151.09, 139.18, 130.61, 129.76, 128.16, 127.14, 111.95, 84.83, 65.38, 56.84, 36.97, 31.91, 29.69, 29.34, 28.58, 25.97, 22.68, 14.11 ppm; ESI-MS $m/z$ 1211.9 (M$^+$), 1234.1 (M + Na$^+$), 2445.4 (M + M + Na$^+$); C$_{74}$H$_{106}$N$_4$O$_{10}$: calcd C, 73.48, H, 8.67, N, 4.63; found: C, 73.35, H, 8.82, N, 4.62.

**Sample Preparation for the DSC, PM, and XRPD Experiments.** Approximately 5−10 mg of a clip or host−guest complex was used in the DSC experiments. In the case of host−guest complexes, an amount of 5−10 mg of clip and an equimolar quantity of guest were dissolved in a mixture of CHCl$_3$ and MeOH (4:1, v/v). The solvent was evaporated overnight under a stream of nitrogen while heating the mixture on a water bath at 40 °C. Samples were prepared in stainless steel large volume pans (75 $\mu$L). All transition temperatures and enthalpies were determined from the first cooling and second heating scans. Polarizing microscopy was carried out under crossed polarizers on a Jeneval polarizing optical microscope connected to a Linkam THMS hot stage. Differential scanning calorimetry thermograms were recorded on a Perkin-Elmer DSC 7 instrument. X-ray powder diffraction experiments were carried out on powdered samples in a pinhole camera (Anton-Paar) operating with a Ni-filtered Cu$_{K\alpha}$ beam. The samples were held in Lindemann glass capillaries (1 mm diameter), and the X-ray patterns were collected on a flat photograpic film.

**Sample Preparation for the FTIR Experiments.** Stoichiometric quantities of the clip and the relevant guest were thoroughly mixed and then ground together with KBr before being pressed as disks. Spectra of the clip and the complexes were recorded before and after heating the pressed disks above the isotropisation temperatures and subsequent cooling. Alternatively, the clip and complexes were melted and cooled on a gold covered microscope slide, and spectra were recorded

(26) CHARMm version 22.0, Revision 92.0911, Resident and Fellows of Harvard College, 1984, 1992, with the use of template charges.
(27) Sijbesma, R. P.; Nolte, R. J. M. *Recl. Trav. Chim. Pays-Bas* **1993**, *112*, 643.

by grazing incidence angle FTIR. In either case the spectra were identical.

**Supporting Information Available:** Crystal data for **2**,[28–31] optical textures of **4** and **5**, and XRPD data for **4** and **5**

and the host−guest complexes of **5**. This material is available free of charge on the Internet at http://pubs.acs.org.

(28) North, A. C. T.; Philips, D. C.; Mathews, F. S. *Acta Crystallogr.* **1968**, *A24*, 351.

(29) De Gelder, R.; de Graaff, R. A. G.; Schenk, H. *Acta Crystallogr.* **1993**, *A49*, 287.

(30) Sheldrick, G. M. SHELXL-97. Program for the refinement of crystal structures; University of Gottingen: Germany, 1997.

(31) Spek, A. L. *Acta Crystallogr.* **1990**, *A46*, C-34.